

## **A MATCHED TRIAXIAL DEVICE FOR CABLE SHIELDING MEASUREMENTS**

**S. Sali**

Department of Electrical, Electronic and Computer Engineering  
University of Newcastle  
Newcastle upon Tyne NE1 7RU, UK

**Abstract**—A matched triaxial device is designed and constructed to measure the transfer impedance of braided coaxial cables at UHF frequencies. Full design principles of the device have been theoretically developed and the details were given in the paper. The device is particularly suited for accurate measurements of transfer impedances at higher radio frequencies up to 3.8 GHz, for which no comparable technique exists. The performance of the device is evaluated by comparing the results against those obtained from low frequency IEC's triple coaxial apparatus and those obtained by using well known theoretical models.

### **1 Introduction**

### **2 Theory**

- 2.1 Reduction of Coupling Equations for  $Z_T$  Measurements
- 2.2 Matched Triaxial Device

### **3 Design of Matched Triaxial Device**

### **4 Experimental Set Up**

### **5 Results**

### **6 Conclusions**

### **Appendix A. Design Equations for IEC Triaxial Apparatus**

### **Appendix B. Numerical Procedure for Extracting Calibrated $Z_T$ Values from High Frequency Measurements**

### **Appendix C. Theoretical Model for Transfer Impedance**

### **References**

## 1. INTRODUCTION

The recent advances in communication technology have increased the complexity and compactness of the electronic systems which resulted in much increased threat of electromagnetic interferences between the circuits. The current limits on radiated and circuit based interference cover the frequency range up to 1.0 GHz but increased frequency bandwidth demanded in applications such as cellular radio systems are likely to result in the proliferations of the standards to higher frequency bands. Closely related issues on radiated immunity and EMC of electronic systems will likely to require further amendments.

Much work has been carried out to predict the leakage from braided coaxial cables at lower radio frequency range up to 100 MHz, with varying degree of success. With a sufficiently accurate prediction method a manufacturer would be able to assess the EMC design criteria that is best suited to the particular application. Most EMC problems require sufficient protection which may demand high degree of immunity to interference. This requires increased accuracy in the leakage estimation and measurements. With the wider market penetration of the cellular radio systems, the problem of cable and wireless interference at higher UHF frequencies must be properly addressed. This requires accuracy in the prediction of the leakage parameters on which the radiation predictions are based.

The characteristics of leakage from a braided coaxial cable is usually measured in terms of transfer impedance  $-Z_T$  which measures the magnetic field leakage and the transfer admittance  $-Y_T$  which measures leakage of electric field. Usually the transfer impedance is several order higher than the transfer admittance and therefore more important for quantitative determination of shielding effectiveness. Several theoretical models were proposed to calculate the transfer impedances of braided coaxial cables but they often fail to give accurate results due to the complexity of the problem. Since the accurate modeling of shielding effectiveness is debatable the most reliable alternative is to determine the leakage parameters by measurements. Several measurement methods have been offered. These include: the current probe and damp methods, the line injection method, and standard International Electrotechnique Committee's (IEC's) triple coaxial apparatus [1-4]. In the first two methods the cable under test is regarded as the radiating source and it is not shielded. The measurements therefore suffer from radiation and coupling effects from the environment. Since such effects increase with frequency these techniques are totally unreliable at higher frequencies. However the simplicity and cost issues make them more desirable for quick and

less accurate measurement tasks [1]. Current probe and line injection techniques do not produce reliable measurements as they do not cover overall sample length and require several repeats in measurements over different lengths along the sample.

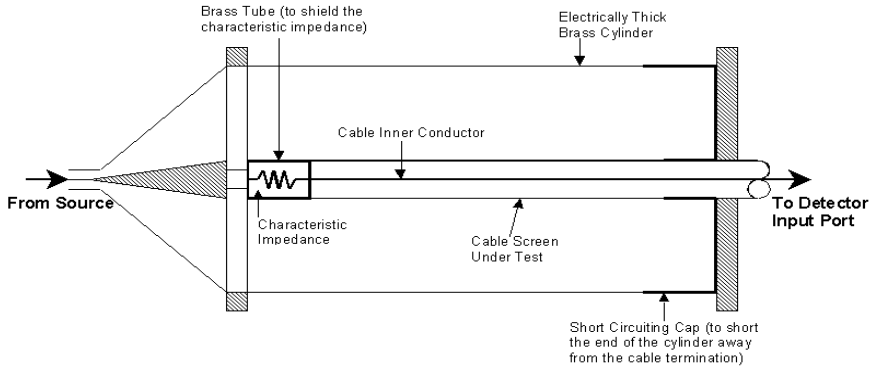


**Figure 1.** Schematic representation for IEC's triple coaxial apparatus.

A standard IEC's triple coaxial apparatus is shown in Fig. 1. In this case the electromagnetic coupling environment is well defined as the cable under test is properly shielded. Therefore this technique yields the most accurate results amongst all the other techniques listed above. However the design of the test procedure is based on the lumped circuit analysis and it can not be extended to higher radio frequencies above 100 MHz. Beyond this limit a new test fixture needs to be designed. Furthermore a coaxial bracket is used to shield a  $47\Omega$  the resistive termination at one end of the test sample. At high frequencies this arrangement causes serious reflections in the sample diluting the accuracy of the measurements. Although it is well established that transfer impedance ( $Z_T$ ) is purely inductive at radio frequencies studies have predicted that it may exhibit nonlinear behavior at very high frequencies [4, 5]. This is due to the following reason.  $Z_T$  is formed of two inductive components: these are called the hole and braid inductances. The hole inductance is responsible for the direct leakage of the internal field to outside through the diamond shaped holes in the braid. Where as the braid inductance is the direct result of magnetic flux linkage in the holes between the braid spindles [6, 7]. It is predicted that at higher radio frequencies the contact resistances between the spindles form reactive impedances which may behave like semi-conducting switches [4]. The braid current therefore may follow lower inductive path and as a result  $Z_T$  may deviate from linear inductive behavior. There is yet no experimental evidence which

has been established to support this prediction although nonlinear harmonic generation from braided coaxial cables were already studied by Benson [7].

The objective of the work presented in this paper is to develop an accurate technique in order to measure the transfer impedance of braided coaxial cables at higher radio frequencies between 300 MHz and 3.8 GHz. A matched triaxial device is designed and successfully employed for this purpose. These measurements may also reveal if the transfer impedance may deviate from a linear behavior beyond a certain frequency limit. The theoretical design details are given fully. The accuracy limits and performance details of the design were assessed both experimentally and with theoretical studies.

## 2. THEORY

The principle of all the measurements involving triaxial configuration is based on triple coaxial arrangement which comprises a thick walled homogeneous brass tube completely enclosing the cable sample with the braided shield. Fig. 1 illustrates the principle, which is theoretically investigated in this section. We consider the most general case for coupling first and reduce the resulting equations to an experimentally convenient arrangement for the accurate measurement of the transfer impedance at higher radio frequencies. Design equations for the low frequency triple coaxial apparatus are also developed for comparison purposes. No electromagnetic coupling is allowed between the inside and outside of the triaxial arrangement. The type of coupling inside the system is represented by the direct crosstalk, which takes place as a consequence of straight energy transmission between the cable under test and the outer tube, and no other intermediary circuit is involved. Fig. 2 shows the per-unit-length equivalent circuit for the triaxial arrangement, where suffices ( $o$ ), ( $s$ ) and ( $i$ ) are used to denote the outer tube, the braided shield and inner conductor of the cable sample respectively. Current and voltages in the outer conductor are denoted by suffix ( $s$ ) and that for the inner conductor by ( $i$ ).  $R$ ,  $L$ ,  $C$ , and  $G$ , in Fig. 2, are the per-unit-length parameters of the respective inner and outer coaxial circuits. The outer coaxial circuit comprises the inner surface of the outer brass tube and the periphery of the outer shield where as the inner coaxial circuit is the coaxial cable under test. The field penetration into the braid, when the outer tube is energized, is represented by discrete equivalent sources which are uniformly distributed along the braid of the sample under test. These sources can be described in terms of the corresponding leakage parameters  $Z_T$  and  $Y_T$ , which refers to the cable sample under test,

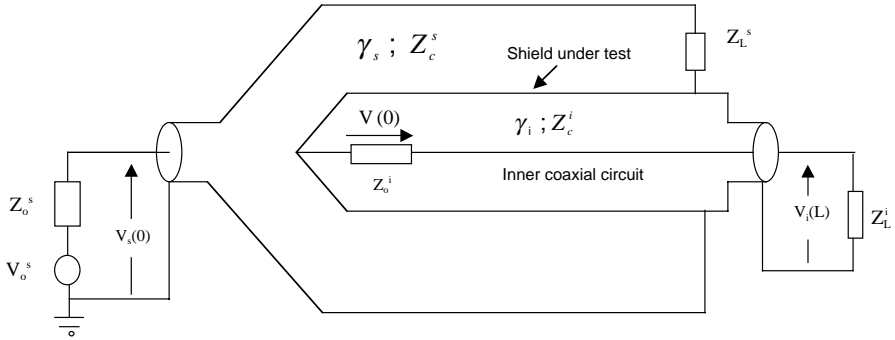


**Figure 2.** Circuit representation of the IEC's triple coaxial arrangement.

as:

$$\begin{aligned} E_T^i(x) &= Z_T I_s(x) \\ I_T^i(x) &= Y_T V_s(x) \end{aligned} \quad (1)$$

where,  $I_s(x)$  and  $V_s(x)$  are the per-unit-length current and voltage in the outer coaxial circuit which is formed between the outer tube and the braided shield of the cable under test. They are defined by the following first order differential equations

$$\begin{bmatrix} \dot{V}_s(x) \\ \dot{I}_s(x) \end{bmatrix} = - \begin{bmatrix} 0 & Z_s \\ Y_s & 0 \end{bmatrix} \begin{bmatrix} V_s(x) \\ I_s(x) \end{bmatrix} \quad (2)$$

The terminal voltage and current inner coaxial circuit are defined by a first order differential equation as:

$$\begin{bmatrix} \dot{V}_i(x) \\ \dot{I}_i(x) \end{bmatrix} = - \begin{bmatrix} 0 & Z_i \\ Y_i & 0 \end{bmatrix} \begin{bmatrix} V_i(x) \\ I_i(x) \end{bmatrix} + \begin{bmatrix} E_T^i(x) \\ Y_T^i(x) \end{bmatrix} \quad (3)$$

where  $Z_s = R_s + j\omega(L_s \mp M_s)$ ,  $Y_s = G_s + j\omega C_s$ ,  $Z_i = R_i + j\omega L_i$  and  $Y_i = G_i + j\omega C_i$ .

The solutions to (2) and (3) is obtained directly by using transmission line approach [6, 9].

$$\begin{aligned} V_s(x) &= \cosh \gamma_s x \cdot V_s(0) - Z_c^s \sinh \gamma_s x \cdot I_s(0) \\ I_s(x) &= -\frac{1}{Z_c^s} \sinh \gamma_s x \cdot V_s(0) + \cosh \gamma_s x \cdot I_s(0) \end{aligned} \quad (4)$$

For the coaxial cable under test the excited terminal voltage and

current in the test cable are described as:

$$\begin{aligned} V_i(x) &= \cosh \gamma_i x \cdot V_i(0) - Z_c^i \sinh \gamma_i x \cdot I_i(0) + \hat{V}_c^i(x) + \hat{I}_s^i(x) \\ I_i(x) &= -\frac{1}{Z_c^i} \sinh(\gamma_i x) \cdot V_i(0) + \cosh(\gamma_i x) \cdot I_i(0) + \hat{V}_s^i(x) + \hat{I}_c^i(x) \end{aligned} \quad (5)$$

where the distributed impressed voltage and current sources which represent the leakage energy from the outer coaxial circuit are represented as:

$$\begin{aligned} \hat{V}_c^i(x) &= \int_0^x \cosh \gamma_i(x - \xi) Z_T I_s(\xi) d\xi \\ \hat{I}_s^i(x) &= -Z_c^i \int_0^x \sinh \gamma_i(x - \xi) Y_T V_s(\xi) d\xi \\ \hat{V}_s^i(x) &= -\frac{1}{Z_c^i} \int_0^x \sinh \gamma_i(x - \xi) Z_T I_s(\xi) d\xi \\ \hat{I}_c^i(x) &= \int_0^x \cosh \gamma_i(x - \xi) Y_T V_s(\xi) d\xi \end{aligned} \quad (6)$$

Inserting (5) into (6) and the resulting equation into (4) we have

$$\begin{aligned} V_i(x) &= \cosh(\gamma_i x) \cdot V_i(0) - Z_c^i \sinh(\gamma_i x) \cdot I_i(0) \\ &+ \frac{1}{(\gamma_s^2 - \gamma_i^2)} \left[ \left( \gamma_s Z_c^i Y_T - \frac{\gamma_i Z_T}{Z_c^s} \right) (\cosh \gamma_s x - \cosh \gamma_i x) \cdot V_s(0) \right. \\ &+ \left\{ Z_T (\gamma_i \sinh \gamma_s x - \gamma_s \sinh \gamma_i) \right. \\ &+ \left. \left. Z_c^s Z_c^i Y_T (\gamma_i \sinh \gamma_i x - \gamma_s \sinh \gamma_s x) \right\} \cdot I_s(0) \right] \end{aligned} \quad (7)$$

$$\begin{aligned} I_i(x) &= -\frac{1}{Z_c^i} \sinh(\gamma_i x) \cdot V_i(0) + \cosh(\gamma_i x) \cdot I_i(0) \\ &+ \frac{1}{(\gamma_s^2 - \gamma_i^2)} \left[ \left\{ \frac{Z_T}{Z_c^s Z_c^i} (\gamma_i \sinh \gamma_s x - \gamma_s \sinh \gamma_i x) \right. \right. \\ &- \left. \left. Y_T (\gamma_s \sinh \gamma_s x - \gamma_i \sinh \gamma_i x) \right\} \cdot V_s(0) \right. \\ &+ \left. \left( \frac{\gamma_i Z_T}{Z_c^i} - \gamma_s Z_c^s Y_T \right) (\cosh \gamma_s x - \cosh \gamma_i x) \cdot I_s(0) \right] \end{aligned} \quad (8)$$

## 2.1. Reduction of Coupling Equations for $Z_T$ Measurements

Equations in (7) and (8) represent the terminal excitation voltage and current in the cable under test in response to electromagnetic leakage from the outer coaxial circuit into the cable. The measurement techniques for the leakage parameters can be derived from these equations by changing the terminal impedances in order to excite the type of coupling required while suppressing the undesired coupling. For example for  $Y_T$  measurements electric field coupling can be excited by an open circuited tertiary in order to enhance shunt voltages in the intermediate circuit and this suppresses the series magnetic currents. On the other hand the measurement of  $Z_T$  requires the opposite: e.g., the use of short circuit to excite the series magnetic current and to suppress the shunt electric voltage in the outer coaxial circuit, which forms the basis of low frequency IEC's triple coaxial apparatus (see Appendix A). At high frequencies open and short circuits cause both instabilities and measurement inaccuracies. In the case of  $Z_T$  measurements in the IEC's triple coaxial apparatus a lumped analysis had to be used in order reduce the general coupling equations to a suitable form from which the measured values can be obtained by simple calculations without measurement inaccuracies. But this reduces the bandwidth of the device to around 100 MHz (sample length less than tenth of a wavelength). Referring to Fig. 2, for the outer coaxial circuit, the terminal conditions in Therein forms are given for a device length  $L$  as

$$V_s(0) = V_o^s - Z_o^s I_z(0) \quad ; \text{ for the outer coaxial circuit} \quad (9)$$

$$V_s(L) = Z_L^s I_s(L)$$

$$V_i(0) = -Z_o^i I_i(0) \quad ; \text{ for the inner coaxial circuit} \quad (10)$$

$$V_i(L) = Z_L^i I_i(L)$$

Substituting (9) into (4) we have

$$I_s(0) = \frac{\left( \cosh \gamma_s L + \frac{Z_L^s}{Z_c^s} \sinh \gamma_s L \right) \times V_o^s}{\left[ \frac{Z_L^s Z_o^s}{Z_c^s} \sinh \gamma_s L + Z_L^s \cosh \gamma_s L + Z_o^s \cosh \gamma_s L + Z_c^s \sinh \gamma_s L \right]}, \quad (11)$$

With the terminal condition described in (9) and (10) equations in (5)

give

$$I_s(0) = \frac{\hat{V}_c^i(L) + \hat{I}_s^i(L) + Z_L^i \hat{V}_s^i(L) - Z_L^i \hat{I}_c^i(L)}{\left[ \frac{Z_L^i}{Z_c^i} \sinh \gamma_i L \cdot Z_o^i + Z_c^i \cosh \gamma_i L + Z_o^i \cosh \gamma_i L + Z_c^i \sinh \gamma_i L \right]} \quad (12)$$

## 2.2. Matched Triaxial Device

The IEC's triple coaxial apparatus employ short circuited outer coaxial line in order to suppress the electric field coupling and enhance magnetic field coupling. This arrangement has the following disadvantages at high frequencies: (i) large measurement errors will result by ignoring electric field coupling, (ii) resonances due to short circuit can not be accurately measured and (iii) resistor bracket is used to house a matching transistor in the inner coaxial line. This arrangement causes large reflections at high frequencies (see Appendix A). Thus a more accurate yet practical technique is needed where the measurement inaccuracies in the existing IEC method can be eliminated. For this it is essential that the short circuit, in the outer coaxial, and the resistive bracket in the inner coaxial circuits are replaced with more stable terminations leading to minimal measurement errors. A practical way to achieve this is to develop a method whereby both circuits are strictly matched, which implies the imposition of the following terminal conditions in the outer and inner lines:  $Z_L^i = Z_o^i = Z_c^i$ ,  $Z_L^s = Z_c^s = Z_o^s$ ,  $Z_c^s = Z_c^i$ . Inserting these into (7) and (8) gives

$$\begin{aligned} \frac{V_i(L)}{V_o^s} &= \left| Y_T Z_c^s - \frac{Z_T}{Z_c^s} \right| \frac{L}{2} \sin c \left( \frac{\beta_s - \beta_i}{2} L \right) \\ \frac{V_i(L)}{V_o^s} &= \left| Y_T Z_c^s + \frac{Z_T}{Z_c^s} \right| \frac{L}{2} \sin c \left( \frac{\beta_s + \beta_i}{2} L \right) \end{aligned} \quad (13)$$

for the far-end and near -end responses of the cable under test. In deriving (13) we have assumed that the attenuation constants of both outer and inner coaxial circuits are small in comparison to the phase constant values.

The main advantage of the matched triaxial device is that both electric field and magnetic field couplings are accounted for, in contrast to IEC's triple coaxial apparatus where the electric field coupling is ignored. Because of this the matched triaxial device is more accurate.

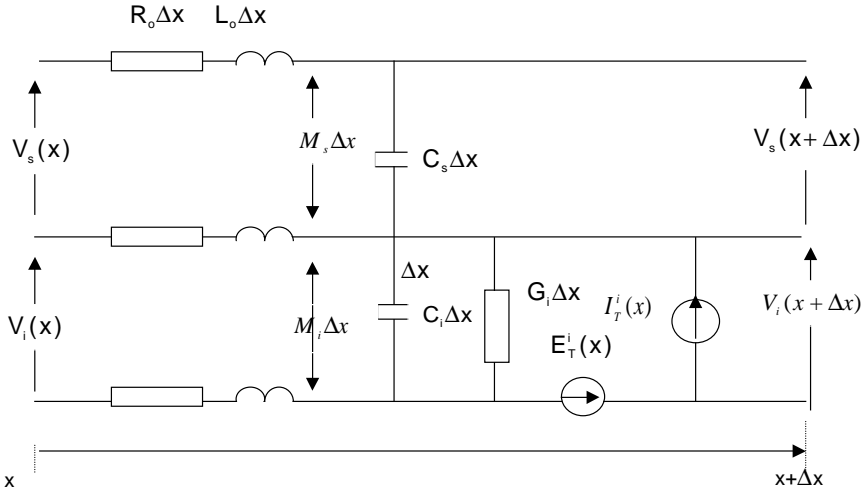


**Figure 3.** The per-unit-equivalent circuit for the triple coaxial apparatus.

### 3. DESIGN OF MATCHED TRIAXIAL DEVICE

The close inspection of expressions in (13) reveal that it is theoretically possible to evaluate both  $Y_T$  and  $Z_T$  values simultaneously if the ‘‘Sinc’’ functions can be eliminated from both expressions. However this is only possible for the far end crosstalk expressions if the phase velocities in the inner and outer coaxial circuits are matched. This enables the transfer impedance values to be extracted from the far-end crosstalk measurements but not from the near end crosstalk for which the ‘Sinc’ function is not eliminated. Thus the design of matched triaxial device is based on matching both the phase velocities and characteristic impedances in the inner and outer coaxial circuits. The outline drawing of the proposed scheme for the device is shown in Fig. 4. Fig. 5 shows the cross-section of the half symmetrical section for the actual device which was constructed and tested. The middle section ‘‘A-B’’ (of length ‘‘L’’) represents the measurement area where the physical coupling between the outer coaxial circuit and the cable sample under test takes place.

The device is designed to measure URM 43 size radio cables (mean diameter over inner dielectric is nominal 3.26 mm). It was necessary to construct the dielectric rods with an inner diameter equal to 3.55 mm in order to protect the braid samples from any deformation. Since any such deformation will cause the braid structure to change  $Z_T$  values

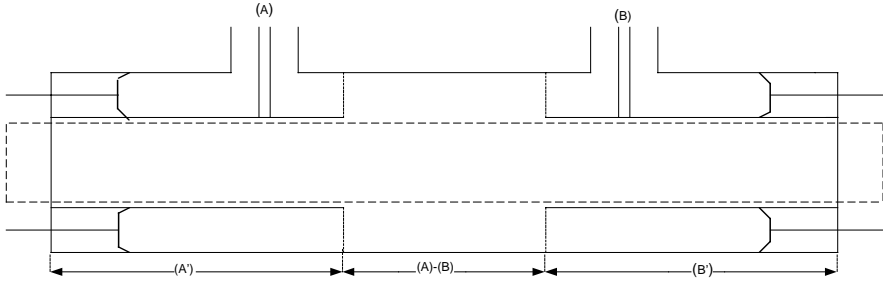


**Figure 4.** The outline drawing for the matched triaxial device.

will also change. A total number of 10 polythene dielectric cylinders of 5.0 cm length enough to fill 0.5 m length are used in the measurement area to match the inner and outer coaxial circuits and the characteristic impedance of different sections was kept nominally 50 ohm throughout the device. With these provisos the inner diameter of the outer tube is obtained as 13.9 mm. A brass tube with the nearest nominal value of 14.1 mm is used. The cable sample from the measurement area is threaded through an inner brass tube. The inner diameter of the tube is determined by the diameter over braid. The thickness of the tube is determined by calculating its outer diameter in conjunction with the inner diameter of the outer tube. A tube of nominal diameter equal to 4.3 mm and thickness of 1.025 mm satisfies the values obtained for the nominal characteristic impedance within the device. The inner tube was sustained coaxially within the device by using a dielectric support with permittivity of 1.6 at both ends (Kraus' optimum compensation matching criteria was used at the end sections of the measurement area [9, 10]). The reactive discontinuities due to changes in the dielectric media are compensated using the short circuiting pistons. Two  $n$ -type receptacles in sections (A)–(B) were kept in position at the 'Junctions' to introduce the signal into and terminate the outer coaxial circuit into the match loads. These Junctions are the main source of discontinuities and were kept apart by a distance equal to the inner diameter of the outer tube in order to ensure that inhomogeneous reactive fields will not interfere with each other. Short circuiting pistons, are made of high conductivity spring fingers in order to provide good metal-to-metal contact. Each piston is provided with fine vernier tuning units for precise movement that is needed at microwave frequencies.

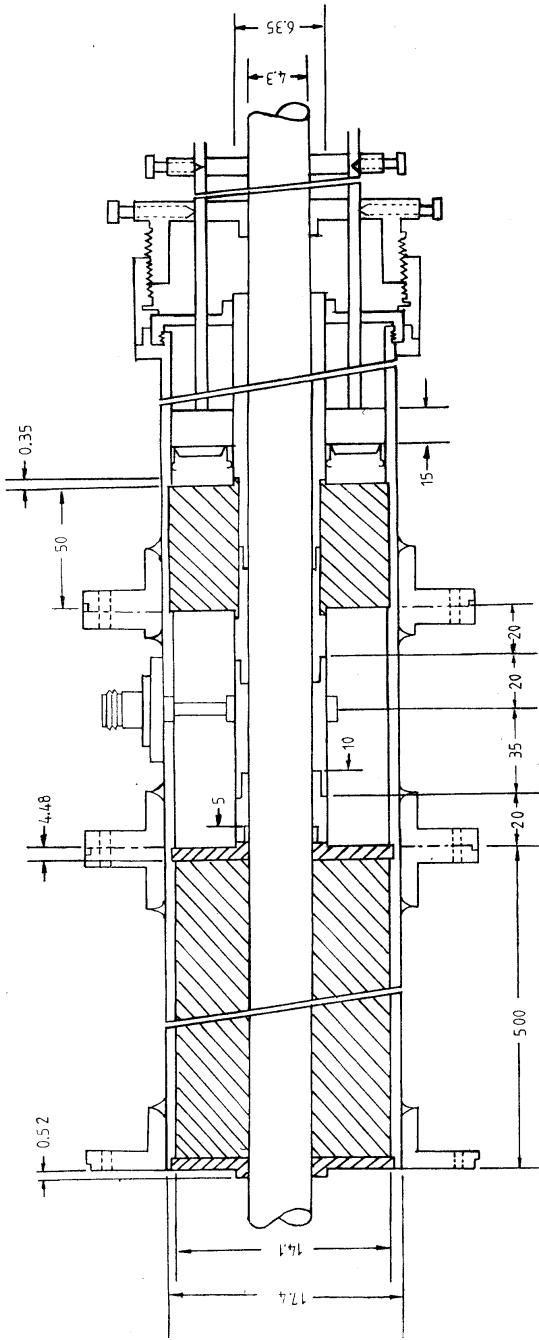
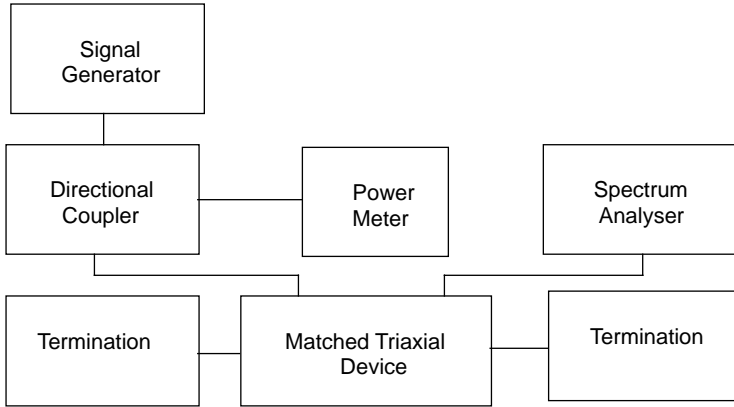
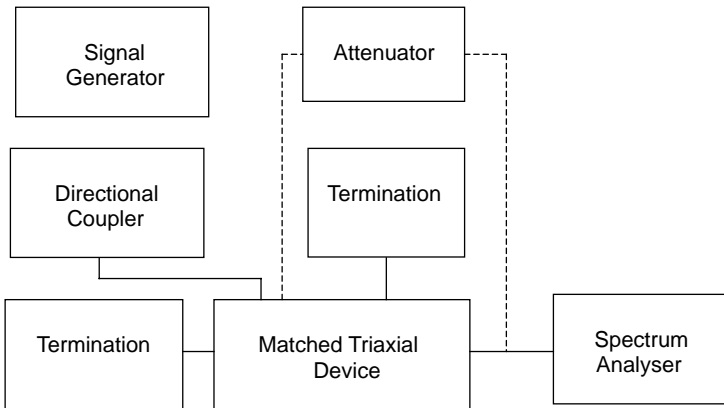


**Figure 5.** Symmetrical half section of the experimental triaxial device with design dimensions (all the dimensions are in mm).



(b) During measurements



(a) During the set up

**Figure 6.** Measurement set up.

#### 4. EXPERIMENTAL SET UP

The experimental set up shown in Fig. 6 is used. The high frequency radio signal is fed at port ( $A$ ) of the device via a bidirectional coupler. An absolute power meter was connected to the coupling output of bi-directional coupler to measure the reflected signal at the input and the port ( $B$ ) is connected the spectrum analyser. The short circuiting stubs were adjusted symmetrically to  $n\frac{\lambda}{4}$ , of the measurement frequency away from the discontinuities at the Junctions. These positions were

monitored alternately until the reflected signal on the power meter was a minimum and the signal on the spectrum analyser was a maximum. At this point the spectrum analyser was disconnected from port ( $B$ ) and connected to the far end of the cable sample and the level of the signal is recorded on the spectrum analyser. The complete assembly was replaced by a set of adjustable attenuators which are then connected between the output of the bidirectional coupler and the input of the spectrum analyser. The settings of the attenuators were adjusted to obtain the same signal level on the spectrum analyser as was obtained with the assembly connected. The transfer impedance of the cable sample at the test frequency was then obtained from the attenuator settings according to equation in (13). Transfer admittance values needed in these expressions were obtained separately by using a pulse method developed by Fowler [6, 11], employing the low frequency IEC's triple coaxial apparatus. As proposed by Tyni [12], for braid angles less than  $45^\circ$  the hole and braid inductances oppose each other. It is therefore possible to determine which inductance predominates for any cable sample examined. A time domain method developed by Fowler [4] is used to perform the polarity tests. The IEC triaxial device was also used for these tests and the procedure is described in detail in [6, 9].

## 5. RESULTS

The magnitude of transfer impedance was measured in the frequency range 300 MHz and 3.8 GHz. The lower frequency cut-off is decided by the size of the short circuiting pistons. It is theoretically possible to lower the frequency range down to 100 MHz but this would require longer device lengths which are not practical. Upper frequency range on the other hand is decided by the diameter of the cable under test. Beyond 4.2 GHz higher order modes will be excited in device [10–13]. The results obtained by using the procedure outlined in Section 4 are shown in Figs. 7–9. The mechanical and electrical details of the cable sample studied are given in Table 1. For each cable sample a comparison is also made between the measurements from the matched triaxial device and those from IEC's triple coaxial apparatus which were shown up to 100 MHz. The theoretical predictions by using the Tyni's theory (see Appendix C) were also shown in solid lines in each graph. It is widely assumed that  $Z_T$  is purely inductive at high frequencies but separate studies predicted that the currents in the braid spindles may follow lower resistive paths because of the increased ac resistances at the cross overs leading to a nonlinear  $Z_T$  behaviour [4, 5]. However the results in Figs. 7–9 clearly indicate that the linear inductive behaviour

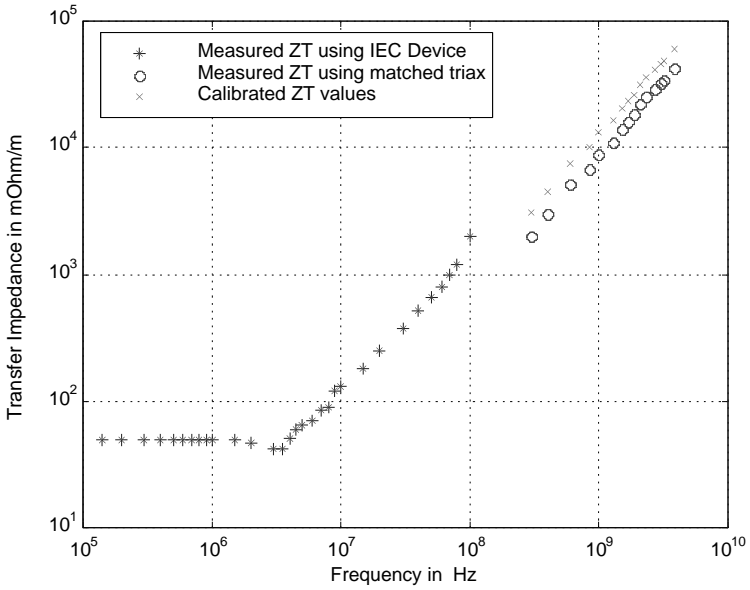


**Figure 7.** Measured  $Z_T$  for HLE 45/1 cable.

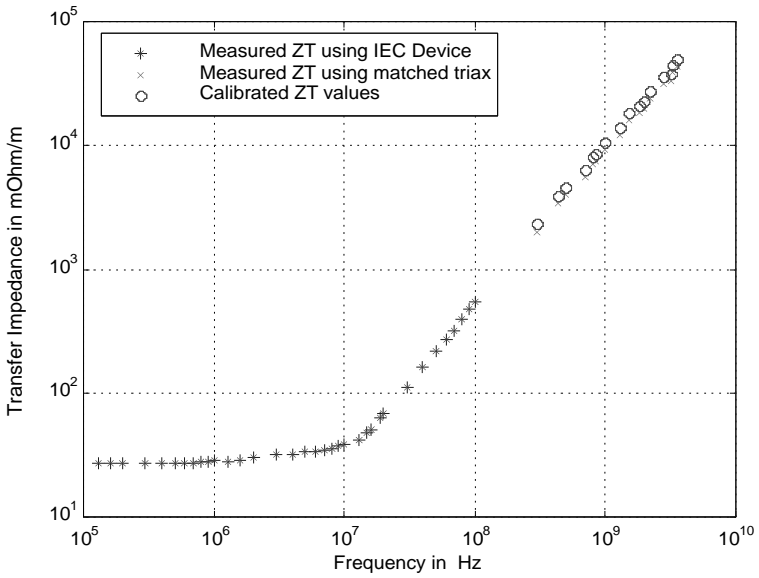


**Figure 8.** Measured  $Z_T$  for HLE 45/2 cable.

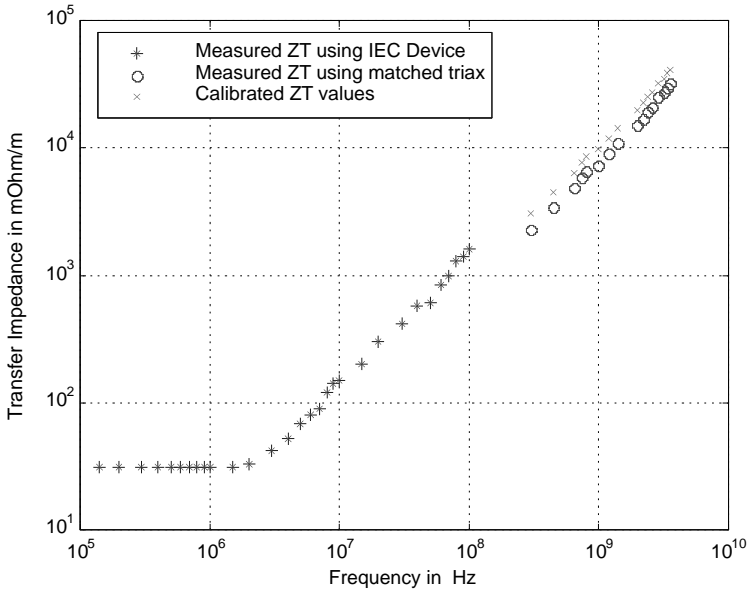


**Figure 9.** Measured  $Z_T$  fo HLE 45/3 cable.

of the  $Z_T$  is preserved well into lower microwave frequencies. A simple frequency extrapolation of the low frequency results to high frequency range indicates approximately 20% discrepancy between the high and low frequency measurements for the two samples HLE 45/1 and HLE 45/3 and around 10% for the other sample HLE 45/2. The results from all the samples tested indicate lower transfer impedance values from matched triaxial device compared to those from low frequency device. A possible explanation for this discrepancy may be due to the changes in the mean distance between the spindles in the braid as p.v.c jacket had to be removed for the high frequency measurements (to match the phase velocities), in contrast to low frequency measurements, where the p.v.c jacket was left in place. The mean distance between the braid spindles directly determines the braid inductance values and any changes in its value is bound to effect the braid inductance values significantly. All the measured samples are of optimised structure (hole and braid inductances are finely balanced by a careful design of filling factor) with positive polarities (hole inductance dominates). Thus  $Z_T$  values are critical to changes in the braid design [12]. Also the release of tension effects the contact resistances at the cross-overs which may result in different current flow between the spindles. Different current flow in the lower spindles will result in different flux coupling in the

**Table 1.** Electrical and mechanical properties of the cable samples measured.

PHYSICAL/ELECTRICAL FEATURES	HLE45/1	HLE45/2	HLE45/3
Sample length (m)	0,5	0,5	0,5
Diameter of inner conductor (mm )	0,9	0,9	0,9
Diameter over dielectric (mm)	2,95	2,95	2,95
Braid wire diameter (mm)	0,1	0,096	0,1
Lay length of cable (mm)	23	23,2	23
Filling factor of cable	0,5283	0,5919	0,44
Braid factor of cable	2,82835	2,51708	3,39595
Inner diameter of dielectric rod (mm)	3,55	3,55	3,55
Outer diameter of dielectric rod (mm)	14,1	14,1	14,1
Loss angle of capacitance	0,0002	0,0002	0,0002
AC resistance of inner line (m $\Omega$ /m)	0,782064	0,695993	0,939010
AC resistance of outer line (m $\Omega$ / m)	0,198048	0,176971	0, 237793
Conductance of inner line (pSiemens/m)	0,021059	0,021059	0, 021059
Conductance of outer line (pSiemens/m)	0,017485	0, 017424	0,017485
Inductance of inner line ( $\mu$ H/m)	0,237433	0,237433	0,237433
Inductance of outer line ( $\mu$ H/m)	0,285956	0,285966	0,285956
Capacitance of inner line (pF/m)	105,293472	105,293472	105,293472
Capacitance of outer line (pF/m)	87,426608	87,118912	87,426608
Capacitance of outer air-gap line (pF/m)	52,979792	52,725888	52,979792

areas between the spindles resulting in the different braid inductance values. These observations may explain the lower discrepancy for the HLE 45/2 cable which has a higher filling factor and therefore more rigid braid construction than other two cables. Overall these effects are impossible to model and more investigations were therefore carried out on the device performance, in order to eliminate further the possible causes that may contribute to the discrepancy. The VSWR measurements give 1.0529 for the inner and 1.1479 for the outer coaxial lines which are pretty close to ideal values. Attenuation constants for the same lines are 0.31899 and 0.067175 dB/m respectively. The transfer impedance values in Figs. 7–9 were obtained from (13) assuming perfect phase velocity match between the inner and outer coaxial circuits. This is not strictly true as there is bound to be air gap between the braid and outer dielectric cylinder sections, in addition to infinitesimal gaps between them. The overall effect of this is to lower the phase constant in the outer coaxial circuit. Therefore we investigated the effect of

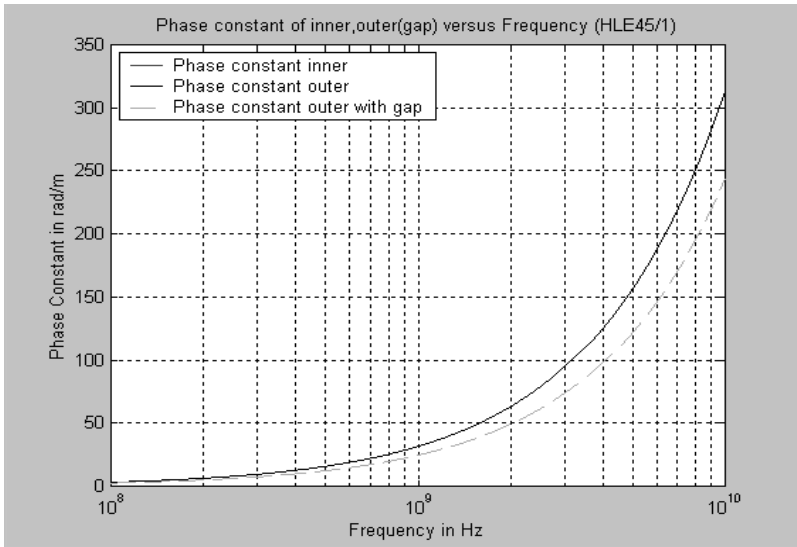


**Figure 10.** Phase velocity with and without the air-gab.

mismatches by assuming that the far end “Sinc” function in (13) is not equal to unity but calculated by assuming an air gap between the outer braided conductor and the dielectric cylinders. The new phase coefficient values were then determined from new capacitance values in the outer coaxial circuit taking into account of this air gab. In Fig. 10 the phase velocity of the inner line is compared with the phase velocity of the outer line with and without the air gab. From the relevant graphs it is seen that the error is negligible between 100 and 400 MHz but increases gradually with frequency. The near- and far-end “Sinc” function are then calculated with the phase error caused with the air gab. These results are shown in Figs. 11 and 12 for the cable samples HLE 45/1. The near-end sinc function was calculated for comparison purposes as it shows highly oscillatory behaviour in comparison to far-end sinc function which smoothly decreases as the frequency increases. This is further illustrated in polar form in Fig. 13. These results also show that it would be impossible to use near-end coupling values in (13) to extract the  $Z_T$  values. The new values of  $Z_T$  calculated including the air-gab from the far-end crosstalk expression in (13) did not show a significant difference. Further investigations concentrated on minimising the mean square error between the extrapolated  $Z_T$  values from the IEC’s device and those from the matched triaxial in order to establish the optimum capacitance values for the outer coaxial circuit.

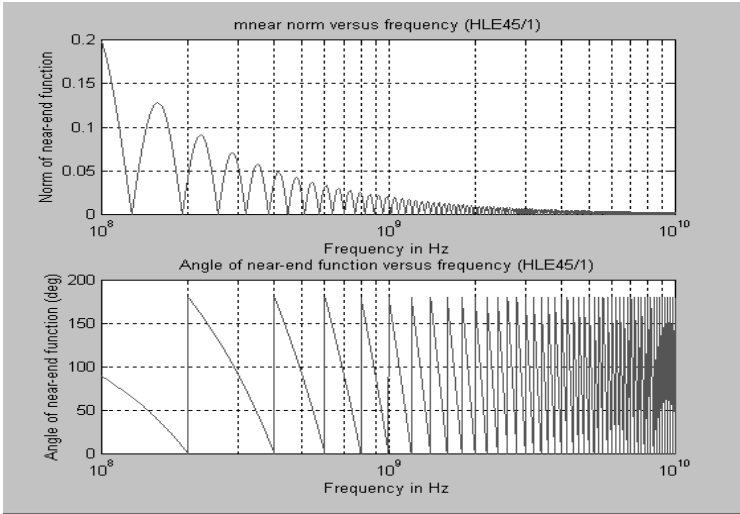


Figure 11. Near end crosstalk with air-gap.

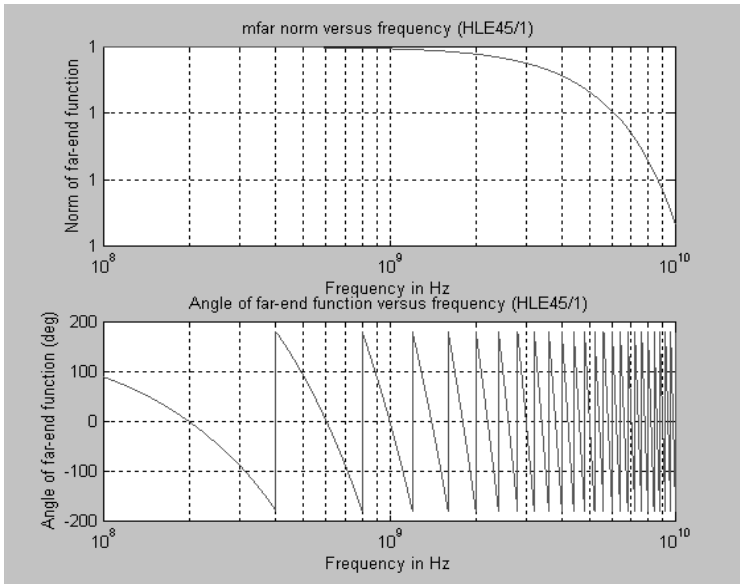
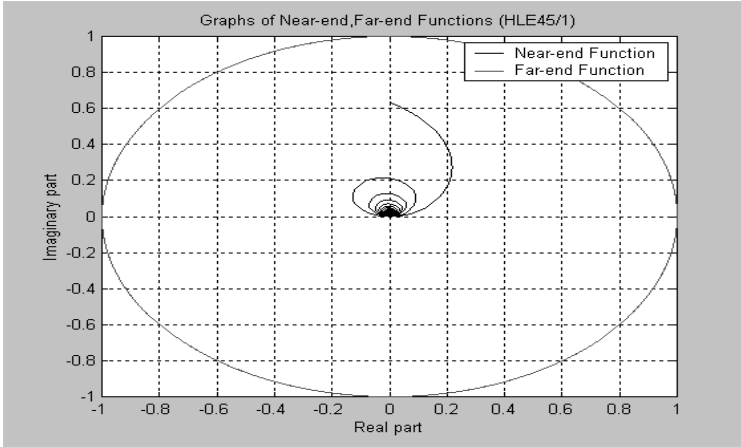


Figure 12. Far end crosstalk values with an air-gap.



**Figure 13.** Polar plots for near and far end crosstalk values.

These values were further inserted into far-end crosstalk expression to re-evaluate the  $Z_T$ . The mathematical details of the approach are given in the Appendix B. The results obtained using this approach (also plotted on the same graphs) show marginally better agreement with those from the low frequency measurements but the discrepancy energy collected from the samples measured. Therefore the discrepancy between the results using two sets of measuring apparatus can be attributed to the sample preparation and the changes in the braid design as a result of removing p.v.c jacket, which alters the interlayer distances between the braid spindles, resulting in modified  $Z_T$  values. The effect is more pronounced on the optimised cable designs as explained above for these cables the hole and braid inductances are finely balanced making them more sensitive to changes in the braid structures.

## 6. CONCLUSIONS

A matched triaxial device was designed and constructed to measure the transfer impedances of braided coaxial cables at higher radio frequencies. Extensive further tests have been carried out in order to investigate the performance characteristics of the constructed device. These tests have proven that the device performed in accordance with the design specifications and it was successful in accurately measuring transfer impedances up to 3.8 GHz. Albeit it requires the removal of dielectric jackets which is a practical disadvantage. Some earlier

studies predicted that transfer impedance may behave nonlinearly at very high frequencies. But these measurements confirmed that the transfer impedance is linear up to 3.8 GHz. However it is interesting to see if the linear behaviour of transfer impedance is sustained up to much higher frequencies into mm-wave region. The design principles of matched triaxial device may easily be applied to extend the frequency limit. However this requires the manufacture of much smaller test cables and device dimensions which will demand greater accuracy in the design and testing.

## APPENDIX A. DESIGN EQUATIONS FOR IEC TRIAXIAL APPARATUS

In the IEC triple coaxial apparatus the outer circuit is shorted at the far end whereas the near end is matched into a 47 ohm resistor enclosed within a metallic bracket. The inner coaxial circuit is matched at both ends. The terminal conditions for the outer line are:  $Z_L^s = 0$ ,  $Z_o^s = Z_c^s$ ,  $Z_L^i = Z_o^i = Z_c^i$ . Inserting these equation in (11) we have

$$I_s(0) = \frac{\cosh \gamma_s L}{[Z_o^s \cosh \gamma_s L + Z_c^s \sinh \gamma_s L]} \cdot V_o^s \quad (\text{A1})$$

Inserting (A1) into (3) and noting that  $V_s(0) = Z_L^s I_s(0)$  for the far end response in the cable we obtain

$$V_i(0) = \frac{1}{(\gamma_i^2 - \gamma_s^2)} \left[ \frac{Z_T}{2Z_c^s} \cdot \frac{\gamma_i(\cosh \gamma_i L + \sinh \gamma_i L - \cosh \gamma_i L) - \gamma_i \sinh \gamma_s L}{\left[ \frac{Z_o^s}{Z_c^s} \cosh \gamma_s L + Z_L^s \sinh \gamma_s L \right] (\cosh \gamma_i L + \sinh \gamma_i L)} \right. \\ \left. - \frac{Y_T Z_c^i}{2} \cdot \frac{\gamma_i(\cosh \gamma_i L + \sinh \gamma_i L - \cosh \gamma_s L) - \gamma_i \sinh \gamma_s L}{\left[ \frac{Z_L^s Z_o^s}{Z_c^s} \sinh \gamma_s L + Z_L^s \cosh \gamma_s L + Z_o^s \cosh \gamma_s L + Z_c^s \sinh \gamma_s L \right]} \right] \\ \cdot V_o^s \quad (\text{A2})$$

Usually the transfer admittance will be small when the outer coaxial line is short circuited (i.e.,  $Z_c^s \sim 0$ ) and  $Z_c^s Z_c^i Y_T \ll Z_T$ . However this is only applicable at low frequencies. As the frequency increases the outer coaxial circuit can only be described in terms of distributed circuit parameters and capacitive coupling creeps into the measurements.

This limits the bandwidth of the triple coaxial apparatus. Thus at low frequencies (A2) is reduced to

$$V_i(L) = \frac{1}{(\gamma_i^2 - \gamma_s^2)} \left[ \frac{Z_T}{2Z_c^s} \cdot \frac{\gamma_i(e^{\gamma_i L} - \cosh \gamma_i L) - \gamma_i \sinh \gamma_s L}{\left[ \frac{Z_o^s}{Z_c^s} \cosh \gamma_s L + Z_L^s \sinh \gamma_s L \right] e^{\gamma_i L}} \right] \cdot V_o^s \quad (\text{A3})$$

At low frequencies  $\alpha_s < \beta_s$  and  $\alpha_i < \beta_i$  (A3) further reduces to a form from which transfer impedance may be evaluated:

$$Z_T = 2 \left| \frac{V_i(L)}{V_o^s} \right| \cdot \frac{R_v}{L} \left[ \frac{(\eta^2 - 1)\chi \left( \sqrt{\cos^2 \chi + \kappa^2 \sin^2 \chi} \right)}{\sqrt{\eta^2 (\cos n\chi - \cos \chi)^2 + (\sin \chi - \eta \sin n\chi)}} \right] \quad (\text{A4})$$

where  $\kappa = \frac{Z_c^s}{R_v}$ ,  $\eta = \frac{\beta_s}{\beta_i}$ ,  $\chi = \beta_i L$  and  $R_v$  represents the series resistance used to match the inner coaxial circuit for the test sample. The second term in the expression above represents the correction factor due to the short circuit employed in the outer coaxial line, to enhance magnetic coupling whilst suppressing the electric field coupling. At low frequencies, where the sample length is electrically short the lumped circuit approximation invoked to derive (A4) will suffice. However as the frequency increases lumped circuit approximation will not be accurate to represent the measurement environment and measurement errors will be introduced in the correction factor. Thus the bandwidth of the triple coaxial apparatus is typically set to 100 MHz for sample lengths around 1 m.

## APPENDIX B. NUMERICAL PROCEDURE FOR EXTRACTING CALIBRATED $Z_T$ VALUES FROM HIGH FREQUENCY MEASUREMENTS

The measured values for the transfer impedance are extracted from the far field crosstalk expression which is re-written here as:

$$\mathfrak{S} = \left[ Y_T Z_c^s - \frac{Z_T}{Z_c^s} \right] \frac{L}{2} \varphi_F(\beta_1, \beta_2)$$

and for near-end crosstalk expression as:

$$N = \left[ Y_T Z_c^s - \frac{Z_T}{Z_c^s} \right] \frac{L}{2} \varphi_N(\beta_1, \beta_2) \quad (\text{B1})$$

where the near and far-end Sinc functions are represented as:

$$\varphi_F(\beta_s, \beta_i) = \sin c \left[ \frac{\beta_s - \beta_i}{2} L \right] \quad \text{and} \quad \varphi_N(\beta_s, \beta_i) = \sin c \left[ \frac{\beta_s + \beta_i}{2} + L \right]$$

The deviation between the low and high frequency measured values of  $Z_T$  can be represented in terms of an error function between the experimental values evaluated via (13) from high frequency triaxial device;  $Z_{TH}$  and that from frequency extrapolated values of transfer impedance from the low frequency triple coaxial apparatus;  $Z_{TL}$

$$e = |Z_{TL} - Z_{TH}| \quad (\text{B2})$$

Since  $Norm \left| Y_T Z_c^s - \frac{Z_T}{Z_c^s} \right| = Norm \left| Y_T + \frac{Z_T}{Z_c^s} \right|$  we can rewrite (B2) as:

$$e = \left| Z_T - Y_T Z_c^s Z_c^i \frac{\varphi_F - \varphi_N}{\varphi_F + \varphi_N} \right| \quad (\text{B3})$$

Minimum mean square norm value in mean square sense can be calculated from  $\frac{\partial |e|^2}{\partial \beta_s} = 0$ , which results in

$$\left( \beta_s^2 - \beta_i^2 \right) \left[ \varphi_n'(\beta_s, \beta_i) \varphi_F(\beta_s, \beta_i) - \varphi_n(\beta_s, \beta_i) \varphi_F'(\beta_s, \beta_i) \right] = 0 \quad (\text{B4})$$

The fundamental solution to (B4) can be obtained as:

$$Ln \left[ \frac{\varphi_F(\beta_s, \beta_i)}{\varphi_n(\beta_s, \beta_i)} \cdot \frac{\varphi_n(\beta_s, 0)}{\varphi_F(0, \beta_i)} \right] = 0 \quad (\text{B5})$$

However this solution refers to the first quadrant in the phase changes, which is not applicable to all frequencies. Thus it is employed as a first estimate in a gradient search technique on (B4) to find the optimum phase constant for the outer coaxial circuit. This value is then used to obtain the new calibrated values of the transfer impedance from the far-end crosstalk measurements according to (B1).

## APPENDIX C. THEORETICAL MODEL FOR TRANSFER IMPEDANCE

The widely used theoretical model for transfer impedance at radio frequencies is due to Tyni [6, 7, 12]. According to this model  $Z_T$  is assumed be inductive at radio frequencies. The inductive rise is made of braid inductance which accounts for the magnetic flux coupling between the braid spindles and hole inductance. The hole inductance is responsible for the direct linkage of the magnetic field via the diamond

shaped holes in the braid to outside and vice-versa. For the per-unit-length braid inductance Tyni suggested

$$M_b = \frac{\mu_o h}{4\pi D_m} (1 - \tan^2 \theta) \quad (\text{C1})$$

For the hole inductance Tyni gave

$$M_h = \frac{\mu_o 2N}{\pi \cos \theta} \left( \frac{b}{\pi D_m} \right)^2 \quad (\text{C2})$$

where  $h$  is the mean distance between the braid spindles,  $D_m$  is diameter of the cable over braid,  $\theta$  is the braid angle,  $N$  is the number of spindles, and  $b$  is the braid wire diameter. It is clear that for braid angles less than  $45^\circ$  hole and braid inductance oppose each other. Thus if the braid inductance is dominant this will result in the polarity change of  $Z_T$  which may be measured by using a simple time domain technique developed by Fowler [1, 9, 11]. This technique is also employed in this paper to determine the polarity of  $Z_T$  for the cable samples measured.

## REFERENCES

1. IEC PUBLICATIONS 96.1, "Screening efficiency," IEC working group doc, No. SE22/A/WG5, Jan. 1967.
2. Fowler, E. P., "Test rings for  $Z_T$  measurements at high frequency," IEC Working Group document, No. SC46/A/WG1 (Fowler 2), November 1973.
3. Martin, A. R. and M. Mendenhall, "A fast accurate and sensitive method for measuring surface transfer impedance," *IEEE Trans.*, Vol. EMC-26, 66-70, 1980.
4. Madle, P. J., "Contact resistances and porpoising effects in braided shields," *IEEE Trans.*, Vol. EMC-23, No. 1, 231-236, March 1980.
5. Goldberg, J. L. and R. J. Slaughter, "Braid construction and attenuation of coaxial cables at microwave frequencies," *Proc. IEE*, Vol. 113, No. 6, 384-389, June 1966.
6. Sali, S., "Coupling problems in a system of multicoaxial cables in homogeneous and inhomogeneous medium," Ph.D. Thesis, Department of Electronics and Electrical Eng., University of Sheffield, UK, Oct. 1982.
7. Tyni, M., "The transfer impedance of coaxial cables with braided conductors," *EMC Symposium*, 423-427, Wroclaw, Poland, Sept. 22-24, 1976.

8. Bayrak, M. and F. A. Benson, "Intermodulation products from nonlinearities in transmission lines at microwave frequencies," *Proc. IEE*, Vol. 122, No. 4, 361–367, April 1975.
9. Sali, S., "Screening efficiency of triaxial cables with optimum braided shields," *IEEE Trans.*, Vol. EMC-42, 26–33, August 1991.
10. Kraus, A., "Reflection coefficient curves of compensated discontinuities on coaxial line and determination of optimum dimensions-Part II," *Journal of British Inst. of Radio Eng.*, Vol. 5, 365–372, May 1962.
11. Fowler, E. P., "Observations on the use of  $Z_T(C)$  for comparing the breakthrough capacitance of cable braids," IEC Working Group document No. SC46/A/WG1 (Fowler 3), November 1973.
12. Homann, E., "Geschirmte kabel mit optimalen gelectschirmen," *Nachrichtentechnische Zeitschrift*, Vol. 21, No. 3, 155–161, 1968.
13. Schelkunoff, S. A., "The electromagnetic theory of coaxial transmission lines and cylindrical shields," *Bell System Technical Journal*, Vol. 13, No. 4, 532–578, October 1934.

**S. Sali** graduated from Birmingham University with a honors degree in Electronic Engineering in 1978. He obtained his Ph.D. from Sheffield University in Electromagnetic Compatibility in 1982. He remained in Sheffield as a research fellow until 1988. Currently he holds a personal readership (high frequency communications) in the Department of Electrical and Electronic Engineering at Newcastle University. His areas of interests are: electromagnetic compatibility including ac losses and applications of high TC superconductors, microwave communications and mobile radio systems. He has managed several large research grants from Science Research Council of UK in these areas and currently managing a small group in high frequency communications area. He has organized and chaired sessions in several international conferences as well as presenting invited papers. He is a member of The Electromagnetics Academy. He is a past recipient of Marconi Award of IEE (1985) and a Chartered Engineer. He is a member of IEEE, and head of Communications and Signal Process Group at Newcastle University.